 CMES, vol.94, no.2, pp.119-138, 2013

Thermal Expansion Behavior of Single Helical Clearance Structure

Cao Guohua[1], **Zhu Zhencai**[1], **Peng Weihong**[2], **Wang Jinjie**[1], **Liu Zhi**[1]

Abstract: The single helical structure is twisted by surrounding helical units with clearance or not between two layers. In order to master the thermal expansion behavior, the theory has been developed for the analysis of these helical structures. The previously deduced linear expressions of thermal expansion coefficients for the gapless structure model (GM) is used and the analytical method is applied to the clearance structure model (CM) and clearance-gapless structure model(CGM) under two boundary conditions. For further evaluating the analytical expressions of two models, the finite element models of the single helical structure surrounding by helical units with lang lay and regular lay are established by using the ANSYS software package. The analytical method is consistent with the numerical method by comparison. Thus, the analytical method is applied to analysis CM, GM and CGM. The results show that the thermal expansion coefficients of GM and CGM are the nonlinear function for the parameters of helical angle, but the CM could be approximately considered as linear functions; these coefficients also could be approximately treated as linear functions of the temperature variable coefficient under two boundary conditions; the value of thermal expansion coefficients for CM is less than GM, but values of CGM are related with the parameters of temperature variable coefficient and helical angle. The method of the analysis for thermal expansion behavior of single helical clearance structure is obtained, which is useful to investigate geometric and mechanical behavior of complicated helical structures.

Keywords: Thermal expansion behavior, linearly explicit expression, single helical clearance structure, temperature effect, finite element model

[1] School of Mechatronic Engineering, China University of Mining and Technology, Xuzhou, China.
[2] School of Mechanics and Civil Engineering, China University of Mining and Technology, Xuzhou, China.

1 Introduction

Helical structures such as ropes or cables were widely used in the field of mine, power transmission, transportation, aviation, bridge and architecture. The mechanical behavior of helical structure had been widely studied by theoretical analysis, finite element analysis and experiment[Huang (1978); Hobbs and Raoof (1983); Velinsky (1985); Ramsey (1990); Costello et al (1997); Feyrer (1997); Jiang et al (2000); Nawrocki and Labrosse (2000); Elata et al (2004); Jiang (2008); Usabiaga and Pagalday (2008); Cao et al (2009)]. And the influence on the temperature effect of the rope or cable is investigated in the field of mine and power transmission [Peng et al (2012); Xia (2009)]. In order to master the thermal expansion mechanism of different steel cables, the thermal expansion characteristics of different steel cables were obtained [Sun et al (2011); Chen et al (2011)], and the linearly expressions of thermal expansion coefficients for prestressed single helical structure are deduced [Cao et al (2012)].

Actually, surrounding helical units of helical structure have clearance between the *i*th and the (*i*-1)th layer. In this paper, based on above scholars' research findings, the thermal expansion behavior of single helical clearance structure is investigated under temperature effect, linearly analytical formulas of the axial and rotational thermal expansion coefficients for the clearance model and gapless-clearance model are obtained. In order to compare with the analytical models, the finite element models of the clearance model and gapless-clearance model are established. The analytical method and finite element method for single helical clearance structure are proposed, which are useful to investigate geometric and mechanical behavior of complicated helical structures.

2 Geometric model and hypotheses

The single helical structure is twisted by surrounding helical units. In order to investigate the thermal characteristics of single helical structure, the front three hypotheses of the reference[Cao et al (2012)] are considered, and the other two hypotheses are considered as follows:

(1) The each layer of the helical structure has clearance between the *i*th layer and the (*i*+1)th layer, and the model is defined as the clearance model(CM). Otherwise, the layers of the model have no clearance, which is defined as the gapless model(GM).

(2) The each layer from the *i*th layer to the *j*th layer has no clearance and the other layers have clearance, the model is defined as the clearance-gapless model(CGM).

The three models are depicted in Fig.1, in which r_0 is the radius of the center unit; r_i is the radius for helical units of the *i*th layer; T is environment temperature, the

T_i is the temperature for helical units of the ith layer; $R_i$is the helical radius of the ith layer for the GM, and the ${}^cR_i$ is the helical radius of the CM or CGM.

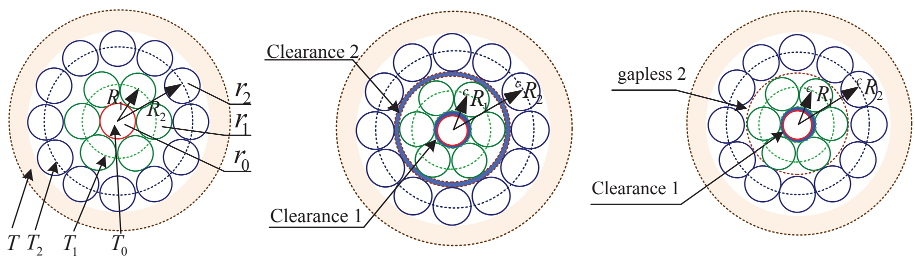

Figure 1: The section of the single helical structure

3 Analytical CM under temperature effect

3.1 The contact force per unit length

The expressions of axial and rotational thermal expansion coefficients for helical structure [Cao et al(2012)]can be formulated as

$$\alpha = \frac{1}{\Delta T}[(1+{}^c\xi_i)\frac{\sin\bar{\gamma}_i}{\sin\gamma_i} - 1],$$

$$\beta = \frac{1}{\Delta T}[\frac{\cot\bar{\gamma}_i}{{}^c\bar{R}_i}(1+\xi_0) - \frac{\cot\gamma_i}{{}^cR_i}],$$

where "$^-$" denotes the variable under temperature effect; $\Delta T_i, \gamma_i$ and ${}^c\xi_i$ are the temperature increment, helical angel and axial strain for helical unit of the ith layer respectively.

By using Taylor Formula, the axial strain ${}^c\xi_i$ and the increment of helical angle $\Delta\gamma_i$for the ith layer could be linearly given as

$${}^c\xi_i = {}^c\tilde{\delta}_i\alpha\Delta T + {}^c\tilde{\zeta}_i\beta\Delta T + {}^c\tilde{\phi}_i\cdot\Delta^cR_i, \tag{1}$$

$$\Delta\gamma_i = {}^c\tilde{\delta}_{\Delta\gamma_i}\alpha\Delta T + {}^c\tilde{\zeta}_{\Delta\gamma_i}\beta\Delta T + {}^c\tilde{\phi}_{\Delta\gamma_i}\cdot\Delta^cR_i, \tag{2}$$

where the coefficient Δ^cR_i is the increment of helical radius ${}^cR_i$, the other coefficients of ${}^c\tilde{\delta}_i, {}^c\tilde{\zeta}_i, {}^c\tilde{\phi}_i, {}^c\tilde{\delta}_{\Delta\gamma_i}, {}^c\tilde{\zeta}_{\Delta\gamma_i}$ and ${}^c\tilde{\phi}_{\Delta\gamma_i}$ are formulated as follows

$${}^c\tilde{\delta}_i = \tan\gamma_i/(\tan\gamma_i+\cot\gamma_i), \quad {}^c\tilde{\zeta}_i = {}^cR_i/(\tan\gamma_i+\cot\gamma_i),$$

$^c\tilde{\phi}_i = -\cot\gamma_i/(^cR_i\tan\gamma_i + {}^cR_i\cot\gamma_i);$

$^c\tilde{\delta}_{\Delta\gamma_i} = (1-{}^c\tilde{\delta}_i)\tan\gamma_i, \quad {}^c\tilde{\zeta}_{\Delta\gamma_i} = -{}^c\tilde{\zeta}_i\tan\gamma_i, {}^c\tilde{\phi}_{\Delta\gamma_i} = -{}^c\tilde{\phi}_i\tan\gamma_i.$

The tension of each helical unit in the single helical structure can be written as $^cF_i = EA_i(^c\xi_i - \alpha_0\varsigma_i\Delta T)$, and could be formulated as

$$^cF_i = {}^c\tilde{\delta}_{F_i}\alpha\Delta T + {}^c\tilde{\zeta}_{F_i}\beta\Delta T + {}^c\tilde{\psi}_{F_i}\alpha_0\Delta T + {}^c\tilde{\phi}_{F_i}\Delta{}^cR_i, \tag{3}$$

in which, $\varsigma_k = \Delta T_k/\Delta T, (k = 0, 1, \ldots, j)$ is the coefficient of temperature increment for helical unit of the kth layer respectively; α_0 is the thermal expansion coefficient of helical unit; coefficients of $^c\delta_{F_i}, {}^c\zeta_{F_i}, {}^c\psi_{F_i}$ and $^c\tilde{\phi}_{F_i}$are written as

$$^c\tilde{\delta}_{F_i} = EA_i{}^c\tilde{\delta}_i,\ {}^c\tilde{\zeta}_{F_i} = EA_i{}^c\tilde{\zeta}_i,\ {}^c\tilde{\psi}_{F_i} = -EA_i\varsigma_i,\ {}^c\tilde{\phi}_{F_i} = EA_i{}^c\tilde{\phi}_i,$$

where E is the elastic modulus of helical unit; $A_i = \pi r_i^2$ is the section area of the helical unit for the ith layer.

According to previously linear method of torsion and bending moment for helical unit relating to the curvatures and the twist [Cao et al (2012)], the expression under temperature effect could be linearly written as

$$^cH_i = {}^c\tilde{\delta}_{H_i}\alpha\Delta T + {}^c\tilde{\zeta}_{H_i}\beta\Delta T + {}^c\tilde{\psi}_{H_i}\alpha_0\Delta T + {}^c\tilde{\phi}_{H_i}\Delta{}^cR_i, \tag{4}$$

$$^cG_i^* = {}^c\tilde{\delta}_{G_i^*}\alpha\Delta T + {}^c\tilde{\zeta}_{G_i^*}\beta\Delta T + {}^c\tilde{\psi}_{G_i^*}\alpha_0\Delta T + {}^c\tilde{\phi}_{G_i^*}\cdot\Delta{}^cR_i, \tag{5}$$

where

$$\begin{aligned}
&^c\tilde{\delta}_{H_i} = C_i\tau_{ai}{}^c\tilde{\delta}_{\Delta\gamma_i},\ {}^c\tilde{\zeta}_{H_i} = C_i\tau_{ai}{}^c\tilde{\zeta}_{\Delta\gamma_i},\\
&^c\tilde{\psi}_{H_i} = C_i\tau_{bi}{}^cR_i\varsigma_i,\ {}^c\tilde{\phi}_{H_i} = C_i(\tau_{ai}{}^c\tilde{\phi}_{\Delta\gamma_i} + \tau_{bi}),\\
&^c\tilde{\delta}_{G_i^*} = B_i\kappa_{ai}{}^c\tilde{\delta}_{\Delta\gamma_i},\ {}^c\tilde{\zeta}_{G_i^*} = B_i\kappa_{ai}{}^c\tilde{\zeta}_{\Delta\gamma_i},\\
&^c\tilde{\psi}_{G_i^*} = B_i\kappa_{bi}{}^cR_i\varsigma_i,\ {}^c\tilde{\phi}_{G_i^*} = B_i(\kappa_{ai}{}^c\tilde{\phi}_{\Delta\gamma_i} + \kappa_{bi}),
\end{aligned}$$

in which $\tau_{ai} = (\cos^2\gamma_i - \sin^2\gamma_i)/{}^cR_i$, $\tau_{bi} = (\sin\gamma_i\cos\gamma_i)/{}^cR_i^2$,

$\kappa_{ai} = -(2\sin\gamma_i\cos\gamma_i)/{}^cR_i, \kappa_{bi} = \cos^2\gamma_i/{}^cR_i^2.$

And coefficients of torsional stiffness C_i and bending stiffness B_i are expressed as

$$C_i = G\pi r_i^4/2, \quad B_i = E\pi r_i^4/4,$$

in which G is the shear modulus.

Based on theory of curve [Love (1944)] and theory of wire rope [Costello (1997)], the shearing force and contact force per unit length was written as ${}^cN_i^* = {}^cH_i\bar{\kappa}_i - {}^cG_i^*\bar{\tau}_i$, ${}^cF_i^* = {}^cN_i^*\bar{\tau}_i - {}^cT_i\bar{\kappa}_i$. And the linear formulates could be written as

$$ {}^cN_i^* = {}^c\tilde{\delta}_{N_i^*}\alpha\Delta T + {}^c\tilde{\zeta}_{N_i^*}\beta\Delta T + {}^c\tilde{\psi}_{N_i^*}\alpha_0\Delta T + {}^c\tilde{\phi}_{N_i^*}\Delta^c R_i, \tag{6} $$

$$ {}^cF_i^* = {}^c\tilde{\delta}_{F_i^*}\alpha\Delta T + {}^c\tilde{\zeta}_{F_i^*}\beta\Delta T + {}^c\tilde{\psi}_{F_i^*}\alpha_0\Delta T + {}^c\tilde{\phi}_{F_i^*}\Delta^c R_i, \tag{7} $$

where

$$ {}^c\tilde{\delta}_{N_i^*} = \kappa_i{}^c\tilde{\delta}_{H_i} - \tau_i{}^c\tilde{\delta}_{G_i^*}, {}^c\tilde{\zeta}_{N_i^*} = \kappa_i{}^c\tilde{\zeta}_{H_i} - \tau_i{}^c\tilde{\zeta}_{G_i^*}, $$

$$ {}^c\tilde{\psi}_{N_i^*} = \kappa_i{}^c\tilde{\psi}_{H_i} - \tau_i{}^c\tilde{\psi}_{G_i^*}, {}^c\tilde{\phi}_{N_i^*} = \kappa_i{}^c\tilde{\phi}_{H_i} - \tau_i{}^c\tilde{\phi}_{G_i^*}; $$

$$ {}^c\tilde{\delta}_{F_i^*} = \tau_i{}^c\tilde{\delta}_{N_i^*} - \kappa_i{}^c\tilde{\delta}_{F_i}, {}^c\tilde{\zeta}_{F_i^*} = \tau_i{}^c\tilde{\zeta}_{N_i^*} - \kappa_i{}^c\tilde{\zeta}_{F_i}, $$

$$ {}^c\tilde{\psi}_{F_i^*} = \tau_i{}^c\tilde{\psi}_{N_i^*} - \kappa_i{}^c\tilde{\psi}_{F_i}, {}^c\tilde{\phi}_{F_i^*} = \tau_i{}^c\tilde{\phi}_{N_i^*} - \kappa_i{}^c\tilde{\phi}_{F_i}, $$

in which $\kappa_i = \cos^2\gamma_i/{}^cR_i$, $\tau_i = (\sin\gamma_i\cos\gamma_i)/{}^cR_i$.

3.2 Linear expressions for axial load and torsion

Because all layers have separated and all helical units could be treated as individual spring, the contact force per unit length ${}^cF_i^*$ of Eq.7 turns out to be zero, namely, ${}^cF_i^* = 0$. The increment of helical radius Δ^cR_i could be deduced as

$$ \Delta^c R_i = {}^c\delta_{\Delta R_i}\alpha\Delta T + {}^c\zeta_{\Delta R_i}\beta\Delta T + {}^c\psi_{\Delta R_i}\alpha_0\Delta T, \tag{8} $$

where ${}^c\delta_{\Delta R_i} = -{}^c\tilde{\delta}_{F_i^*}/{}^c\tilde{\phi}_{F_i^*}, {}^c\zeta_{\Delta R_i} = -{}^c\tilde{\zeta}_{F_i^*}/{}^c\tilde{\phi}_{F_i^*}, {}^c\psi_{\Delta R_i} = -{}^c\tilde{\psi}_{F_i^*}/{}^c\tilde{\phi}_{F_i^*}$.

According to the Eq.8, the ${}^c\xi_i$, $\Delta^c\gamma_i$, ${}^cF_i$, ${}^cH_i$, ${}^cG_i^*$ and ${}^cN_i^*$ could be defined by parameters $\alpha\Delta T, \beta\Delta T$ and $\alpha_0\Delta T$, which are expressed by Eq.A-2$\sim$ Eq.A-7 in Appendix.

Based on the total axial force and torsion expressions listed by Eq.A-8, and Eq.A-2$\sim$Eq.A-7, the total axial force and torsion under temperature effect could be linearly formulated by Eq.A-9 in Appendix.

3.3 Axial and rotational thermal expansion coefficients

In order to obtain linear expressions of axial and rotational thermal expansion coefficients, the two boundary conditions are adopted as follows:

(1) Boundary condition 1(BC1): The axial and rotational movements are restricted at one end of the single helical structure, and movements at the other end are free.

(2) Boundary condition 2(BC2): The axial and rotational movements are also restricted at one end of the single helical structure, but the rotational movement is restricted and the axial movement is free at the other end.

According to BC1, the α and β could be deduced [Cao et al (2012)] and linearly defined as $\alpha = \chi_{(n)}\alpha_0$ and $\beta = o_{(n)}\alpha_0$ by ratios of axial and rotational thermal expansion coefficients $\chi_{(n)}$ and $o_{(n)}$ respectively, which are expressed by Eq.A-12 and Eq.A-13 in Appendix.

Based on the BC2, the only axial thermal expansion coefficient α could be obtained, which is depicted by Eq.A-14, and the axial thermal expansion coefficient $\chi_{(n)}$ is listed by Eq.A-15 in Appendix.

4 Analytical CGM under temperature effect

Because the kth layer is just touching the $(k-1)$th and $(k+1)$th from ith to jth layers, the sum of the contact force per unit length ${}^{c}F_i^*$ of Eq.7 turns out to be zero, namely

$$\sum_{k=i}^{j} m_k {}^{c}F_k^* s_k = 0, \tag{9}$$

where m_k is the total units amount in the kth layer, and the length of the kth layer for helical units s_k, is defined as

$$s_k = \sqrt{p_i^2 + (\theta_k R_k)^2} = p_i / \sin(\gamma_k),$$

where p_i denotes the pitch of the ith layer for helical units;$\theta_k$is the rotation angle of helical units for the kth layer.

And the increment radius of different layers from the (i+1)th to the jth layer could be defined as

$$\begin{cases} \Delta^c R_{i+1} = \Delta^c R_i - \sum\limits_{k=i}^{i+1} (1+\nu) r_k \varsigma_k \alpha_0 \Delta T + \sum\limits_{k=i}^{i+1} \nu r_k {}^{c}\xi_k, \\ \Delta^c R_{i+2} = \Delta^c R_{i+1} - \sum\limits_{k=i+1}^{i+2} (1+\nu) r_k \varsigma_k \alpha_0 \Delta T + \sum\limits_{k=i+1}^{i+2} \nu r_k {}^{c}\xi_k, \\ \quad \vdots \\ \Delta^c R_j = \Delta^c R_{j-1} - \sum\limits_{k=j-1}^{j} (1+\nu) r_k \varsigma_k \alpha_0 \Delta T + \sum\limits_{k=j-1}^{j} \nu r_k {}^{c}\xi_k, \end{cases} \tag{10}$$

in which, ν is the Poisson's ratio for all helical units.

According to Eq.9 and Eq.10, the increment of helical radius $\Delta^c R_k$ could be deduced as $\Delta^c R_k = (\Phi_a^{-1} \cdot \Phi_b \cdot \Phi_c)_k$, and linearly expressed as Eq.8, in which

$${}^{c}\delta_{\Delta R_k} = (\Phi_a^{-1} \cdot \Phi_b)_{k,1}, {}^{c}\zeta_{\Delta R_k} = (\Phi_a^{-1} \cdot \Phi_b)_{k,2}, {}^{c}\psi_{\Delta R_k} = (\Phi_a^{-1} \cdot \Phi_b)_{k,3},$$

where

$$\Phi_a = \begin{bmatrix} m_i\tilde{\phi}_{F_i^*}s_i & m_{i+1}\tilde{\phi}_{F_{i+1}^*}s_{i+1} & m_{i+2}\tilde{\phi}_{F_{i+2}^*}s_{i+2} & m_{i+3}\tilde{\phi}_{F_{i+3}^*}s_{i+3} & \cdots & m_j\tilde{\phi}_{F_j^*}s_j \\ \nu r_i{}^c\tilde{\phi}_i+1 & \nu r_{i+1}{}^c\tilde{\phi}_{i+1}-1 & 0 & 0 & \cdots & 0 \\ 0 & \nu r_{i+1}{}^c\tilde{\phi}_{i+1}+1 & \nu r_{i+2}{}^c\tilde{\phi}_{i+2}-1 & 0 & \cdots & 0 \\ 0 & 0 & \nu r_{i+2}{}^c\tilde{\phi}_{i+2}+1 & \nu r_{i+3}{}^c\tilde{\phi}_{i+3}-1 & \cdots & 0 \\ \vdots & \vdots & \vdots & \vdots & \ddots & \vdots \\ 0 & 0 & 0 & 0 & \cdots & \nu r_j{}^c\tilde{\phi}_j-1 \end{bmatrix}_{(j-i+1)\times(j-i+1)}$$

$$\Phi_b = \begin{bmatrix} -\sum_{k=i}^{j} m_k{}^c\tilde{\delta}_{F_k^*} & -\sum_{k=i}^{j} m_k{}^c\tilde{\zeta}_{F_k^*} & -\sum_{k=i}^{j} m_k{}^c\tilde{\psi}_{F_k^*} \\ -\sum_{k=i}^{i+1} \nu r_k{}^c\tilde{\delta}_k & -\sum_{k=i}^{i+1} \nu r_k{}^c\tilde{\zeta}_k & \sum_{k=i}^{i+1}(1+\nu)r_k\varsigma_k \\ \vdots & \vdots & \vdots \\ -\sum_{k=j-1}^{j} \nu r_k{}^c\tilde{\delta}_k & -\sum_{k=j-1}^{j} \nu r_k{}^c\tilde{\zeta}_k & \sum_{k=j-1}^{j}(1+\nu)r_k\varsigma_k \end{bmatrix}_{(j-i+1)\times 3}$$

$$\Phi_c = \begin{bmatrix} \alpha\Delta T & \beta\Delta T & \alpha_0\Delta T \end{bmatrix}^{\mathrm{T}}$$

According to expressions Eq.1$\sim$ Eq.6, the ${}^c\xi_i$, $\Delta^c\gamma_i$, ${}^cF_i$, ${}^cH_i$, ${}^cG_i^*$ and ${}^cN_i^*$ could be formulated, and the axial and rotational thermal expansion coefficients of CGM could be deduced by Eq.A-2$\sim$ Eq.A-7 in Appendix.

5 The finite element model of single helical structure

In order to evaluate the analytical expressions of two models, the finite element method by the software package ANSYS is adopted. The detailed modeling process is presented as follows:

First, the helical lines are generated in a global cylindrical coordinate system according to the mathematical equation, which is showed by Eq.A-1 in Appendix.

Second, the source areas are meshed using the 2-D MESH200 element contributing nothing to the solution, then dragged along above defined paths forming the whole helical unit by assigning the 3-D SOLID186 element. In addition, the mesh in contact regions of the CGM model is refined to simulate deformation precisely. There are 107785, 294409 and 387721 elements in the 1+6 form of CM, 1+6+12 form of CM and CGM, respectively.

Third, surface to surface contact is defined between center unit and helical units of 1th layer, and between helical units of 1th layer and helical units of 2th layer in GM; surface to surface contact is also defined between 1th layer and 2th layer in CGM. The contact elements TARGE170 and CONTA174 were employed in these models without considering friction coefficients.

Finally, two boundary conditions are utilized to analysis. Note that the source areas are defined as a rigid region. Because the SOLID186 element is lack of rotational degrees of freedom, a point element MASS21 with six degrees of freedom is adopted to couple with all the nodes in rigid regions for measuring the rotational movement.

The model for 1+6 of CM is depicted in Fig.2a, the 1+6+12 of CM and CGM with lang lay and regular lay are showed in Fig.2b and Fig.2c.

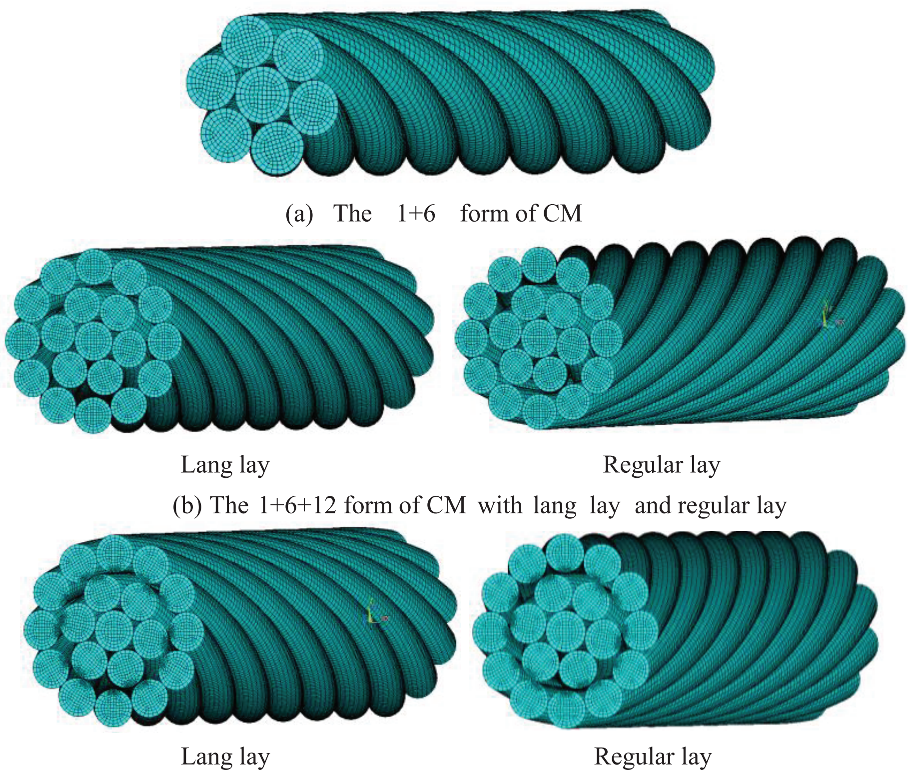

(a) The 1+6 form of CM

Lang lay Regular lay

(b) The 1+6+12 form of CM with lang lay and regular lay

Lang lay Regular lay

(c) The 1+6+12 form of CGM with lang lay and regular lay

Figure 2: The finite element model of single helical structure

6 Result and analysis

6.1 Parameters

In order to compare characteristics of the thermal expansion coefficient among CM, GM and CGM, the parameters of the single helical structures are the same and listed in Table 1. The young's modulus, Poisson ratio and thermal expansion coefficient of helical units are 2.06×10^{11}Pa, 0.3 and $1.2\times10^{-5}/^{o}$C respectively. The length of the single helical structure is 60mm, and the coefficients of temperature increment are defined in Table 2.

Table 1: Geometry parameters of single helical structure

	Geometry parameters						
Forms	Diameter (mm)	r_0 (mm)	r_1 (mm)	r_2 (mm)	γ_1 (°)	γ_2(°) Lang lay	γ_2(°) Regular lay
1+6	5.588	0.990	0.902	/	70	/	/
1+6+12	9.200	0.990	0.902	0.903	70	70	110

Table 2: Coefficients of temperature increment

	Temperature parameters	
Forms	Coefficients	Valves
1+6	ς_0	0.5
	ς_1	1
1+6+12	ς_0	0.5
	ς_1	0.8
	ς_2	1

6.2 Comparison between the analytical and numerical solution

The comparison on the thermal expansion coefficients was analyzed by analytical and FEM methods, and showed in Table 3.

According to Table 3, the comparison with the analytical model and numerical model shows the considerable consistency for two proposed methods of the single helical structure. The relative errors of the axial and rotational thermal expansion coefficient between the analytical solution and the numerical solution are less than 6%, expect the relative errors for the rotational thermal expansion coefficients of CM under BC1(13%), the axial and rotational thermal expansion coefficients of CGM under BC1(11.8% and 13.1% respectively),which is mainly caused by the effect of boundary constraints and contact deformation in the finite element model.

Table 3: Comparison of thermal expansion coefficients

Models	Forms	BC	Methods	Thermal expansion coefficients Axial (10^{-5}/°C)	Rotation (10^{-5}rad/°C)
CM	1+6	1	Analytical solution	0.718	-21.55
			Numerical solution	0.731	-18.75
			Difference	1.8%	13%
		2	Analytical solution	0.718	/
			Numerical solution	0.731	/
			Difference	1.8%	/
	1+6+12 (Lang Lay)	1	Analytical solution	0.722	-11.78
			Numerical solution	0.726	-11.15
			Difference	0.6%	5.3%
		2	Analytical solution	0.723	/
			Numerical solution	0.726	/
			Difference	0.4%	/
	1+6+12 (Regular Lay)	1	Analytical solution	0.723	3.615
			Numerical solution	0.726	3.483
			Difference	0.4%	3.7%
		2	Analytical solution	0.723	/
			Numerical solution	0.726	/
			Difference	0.4%	/
CGM	1+6+12 (Lang Lay)	1	Analytical solution	0.896	194.56
			Numerical solution	0.950	184.88
			Difference	6.0%	5.0%
		2	Analytical solution	1.064	/
			Numerical solution	1.100	/
			Difference	3.4%	/
	1+6+12 (Regular Lay)	1	Analytical solution	0.800	-171.75
			Numerical solution	0.907	-149.29
			Difference	11.8%	13.1%
		2	Analytical solution	1.064	/
			Numerical solution	1.098	/
			Difference	3.2%	/

Therefore, the presented methods of analytical model and numerical model are reasonable, and the two models could be adopted independently to study the behavior of the helical structure.

6.3 Comparison with the GM, CGM and CM

The comparison on the axial and rotational thermal expansion coefficients is analyzed by taking the GM, CGM and CM. The comparison on the ratios of thermal expansion coefficients is showed in Table 4 by taking the geometry parameters of Table 1. The thermal expansion coefficients influenced by ratio of temperature increment and helical angle are shown in Fig.3$\sim$Fig.6 respectively.

Table 4: Comparison of the GM, CGM and CM

Forms	BC	Models	Ratios of thermal expansion coefficients	
			Axial	Rotation
1+6	1	GM	0.826	197.247
		CM	0.599	-17.960
	2	GM	0.936	/
		CM	0.599	/
1+6+12 (Lang Lay)	1	GM	0.767	155.628
		CGM	0.746	162.129
		CM	0.602	-9.812
	2	GM	0.932	/
		CGM	0.886	/
		CM	0.602	/
1+6+12 (Regular Lay)	1	GM	0.868	-98.895
		CGM	0.667	-143.122
		CM	0.602	3.013
	2	GM	0.932	/
		CGM	0.886	/
		CM	0.602	/

According to Table 4, the axial thermal expansion coefficients of CM are nearly the same, and have no relation to the two boundary conditions. The rotational thermal expansion coefficients of CM are less than GM and CGM, and could be treated as zero approximately. Based on Fig.3, with the increase of the ratio for temperature increment ς_1, the thermal expansion characteristics of three models show that: the axial thermal expansion coefficient $\chi_{(n)}$ of GM increases gradually under BC1, while the rotational thermal expansion coefficient $o_{(n)}$ decreases; the average growth rate of $\chi_{(n)}$ for GM under BC2 is lower than that under BC1; both $\chi_{(n)}$ and $o_{(n)}$ of CGM decrease with the raise of ς_1 under BC1, and $\chi_{(n)}$ also decreases under BC2; the $\chi_{(n)}$ of CM increases slowly with the increase of ς_1 under

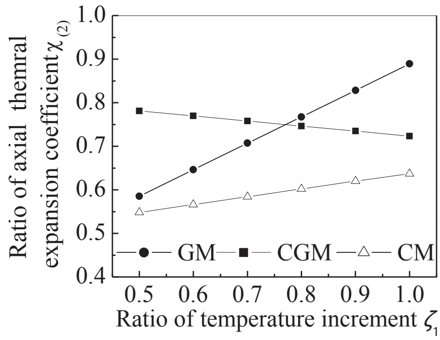

(a) $\chi_{(2)}$ under BC 1

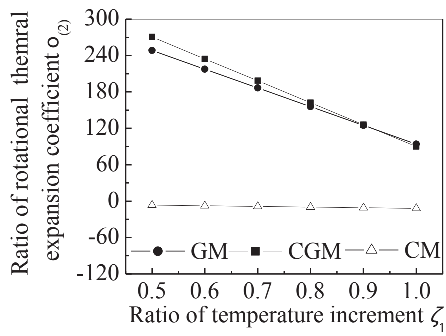

(b) $o_{(2)}$ under BC 1

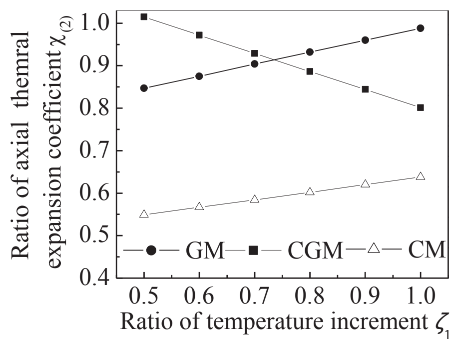

(c) $\chi_{(2)}$ under BC 2

Figure 3: Ratios of thermal expansion coefficients for lang lay influenced by ratio of temperature increment

two boundary conditions, while $o_{(n)}$ is almost unchanged under BC1. Notice that the $\chi_{(n)}$ of CGM is more than GM at the initial stage of ς_1; then the $\chi_{(n)}$ of CGM is decreasing with the increase of ς_1, and the $\chi_{(n)}$ of CGM is less than GM while $\varsigma_1 > 0.76$.

The phenomenon of CM, GM and CGM with the increase of the ratio for temperature increment ς_1 can be described as:

(1)The deformation of helical structure is interacted by different tensions of different spiral twisting units under temperature effect. Because the inner spiral layers have different clearance, the CM, GM and CGM have different contributions on the axial and torsional deformations.

(2) As for CM, each helical unit is independent of each other, which just likes a spring. Since there is no contact force among helical units, the axial stiffness of

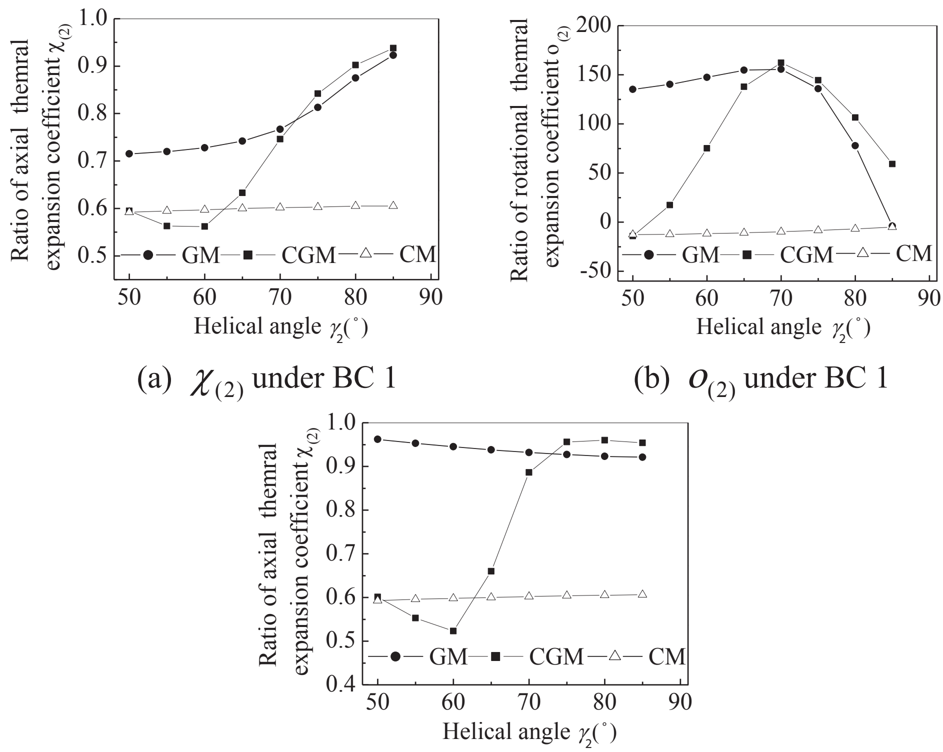

(a) $\chi_{(2)}$ under BC 1

(b) $o_{(2)}$ under BC 1

(c) $\chi_{(2)}$ under BC 2

Figure 4: Ratios of thermal expansion coefficients for lang lay influenced by helical angle

each helical unit is relatively small. Therefore, the axial load and torque is smaller than the GM and CGM under temperature effect. Namely, the $o_{(n)}$ of CM model is near to zero, and the $\chi_{(n)}$ of CM is smaller than GM and CGM.

(3)As for CGM and GM:

(a)while $0.5 < \varsigma_1 < 0.76$, there is a large difference in temperature between inner and outer helical layers. If the temperature drops, outer units' shrinkage is larger in CGM. The outer unit applies a contact pressure to the inner, which makes the inner helical unit develop a bending deformation. Consequently, the axial force of contraction for inner helical units increases. Furthermore, the outer layer suffers counterforce, which also makes the deformation of inward shrinkage decrease, namely, the axial force of contraction for outer helical unit increases. Therefore, axial radios of thermal expansion coefficients of CGM are larger than GM while

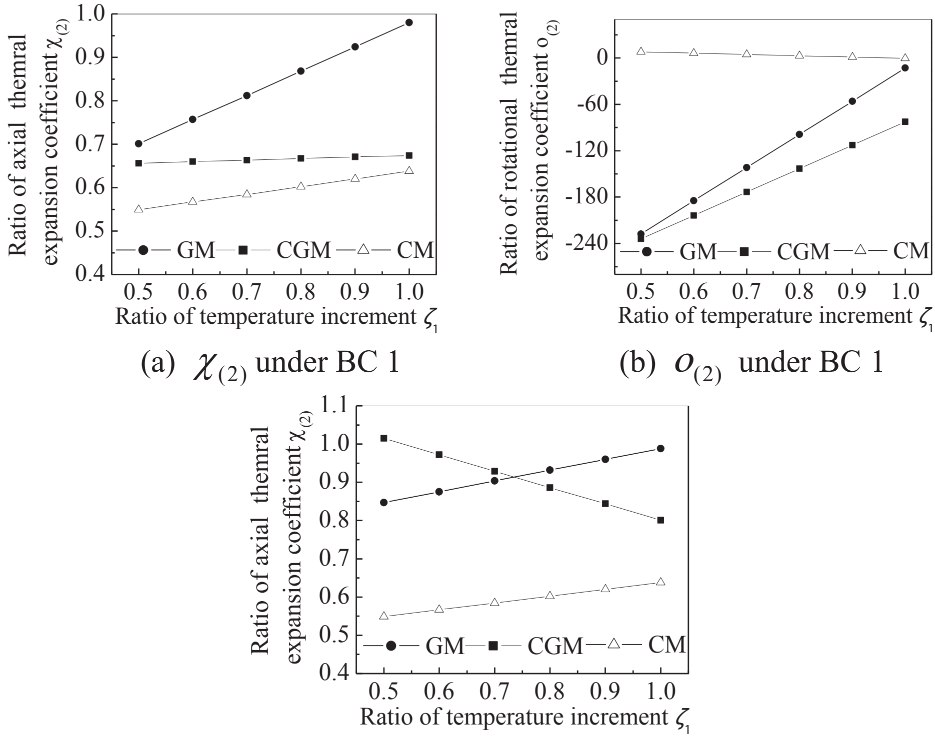

(a) $\chi_{(2)}$ under BC 1 (b) $o_{(2)}$ under BC 1

(c) $\chi_{(2)}$ under BC 2

Figure 5: Ratios of thermal expansion coefficients for regular lay influenced by ratio of temperature increment

0.5< ς_1 <0.76.

(b)While ς_1 >0.76, there is a small difference in temperature between inner and outer helical layers. The ability of contact force and bending deformation declines, and the influence of inner and outer helical layer's axial contraction force becomes weaker. As for GM, the outer helical units' deformation of inward shrinkage is restricted, so the influence of axial force of contraction for the outer helical units becomes relatively stronger. Therefore, axial radios of thermal expansion coefficients of GM are larger than CGM while ς_1 >0.76.

(c)In conclusion, radios of thermal expansion coefficients of CGM model are not always between the GM and CM.

According to Fig.4, the thermal expansion coefficients of GM and CGM are non-linear functions of helical angle γ_2 under two boundary conditions, but thermal

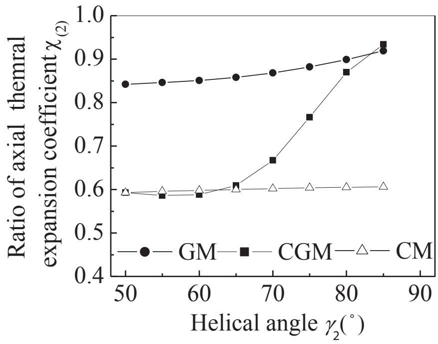

(a) $\chi_{(2)}$ under BC 1

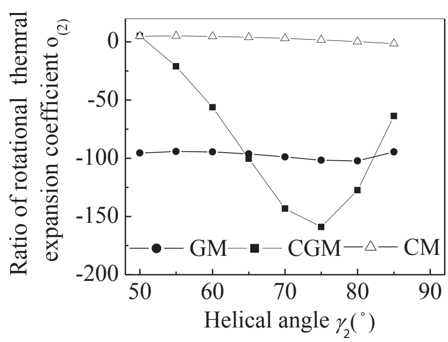

(b) $o_{(2)}$ under BC 1

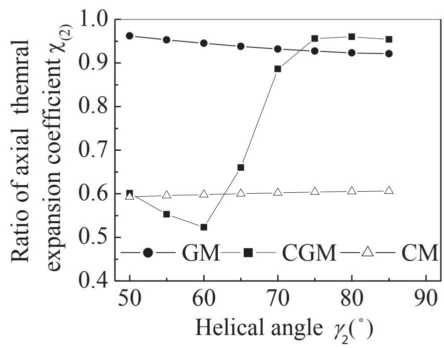

(c) $\chi_{(2)}$ under BC 2

Figure 6: Ratios of thermal expansion coefficients for regular lay influenced by helical angle

expansion coefficients of CM are almost unchanged under two boundary conditions. For the similar reasons, when the helical angle is different, the center unit and outer helical units have different contributions to axial deformation. There is a difference that the CGM's axial radios of thermal expansion coefficients fluctuate when helical angle changes. The length of helical unit s_k decreases when helical angle increases, but contact force is the product of contact force per unit length ${}^cF_k^*$ and axial length of helical unit s_k. Therefore, the contribution to axial deformation changes with the variation of helical angle.

Additionally, the relationship with the regular lay can be clearly found from Fig.5 and Fig.6.

7 Conclusions

The thermal expansion behavior of single helical clearance structure is systematically investigated under temperature effect. Some conclusions are obtained and summarized as follows:

1. The previously deduced linear expressions of thermal expansion coefficients for GM is used and the analytical method is applied to CM and CGM with lang lay and regular lay under two boundary conditions.

2. Linearly explicit expressions of the increment of helical radius for CM and CGM are developed, and the linearly explicit expressions of thermal expansion coefficients for CM and CGM are deduced finally under temperature effect.

3. The finite element models of CM and CGM with 1+6 form and 1+6+12 form surrounding by helical units with lang lay and regular lay are established under two boundary conditions by using the ANSYS software package. The analytical method is consistent with the numerical method by comparison.

4. The analytical method is applied to analysis CM, GM and CGM with lang lay and regular lay, and the thermal expansion characteristics with relation to the parameters of temperature variable coefficient and helical angle are obtained under two boundary conditions.

5. Linearly thermal expansion coefficients of single helical clearance structure is obtained, which is useful to investigate the critical load from CM to GM or geometry change of the spiral wire section in future.

Acknowledgement

This research is sponsored by "National Science Foundation for Young Scientists of China" (Grant No.51005233), and the"A Project Funded by the Priority Academic Program Development of Jiangsu Higher Education Institutions "PAPD".".

References

Cao, G. H.; Zhu, Z. C.; Peng, W. H.; Chen, G. A. (2009): Variations of curvature, torsion and stress of double helix wire in 6×7+IWS wire rope. *Journal of Mechanical Strength*, vol.31, no.3, pp.491-496(In Chinese).

Cao, G. H.; Li, K.; Zhu, Z. C.; Peng, W. H.; Mao, X. B. (2012): Thermal Expansion Characteristic of Prestressed Single Helical Structure. *CMES-Computer Modeling in Engineering & Sciences,* vol.83, no.4, pp.403-423.

Chen, Z. H.; Liu, Z. S.; Sun, G. J. (2011): Thermal behavior of steel cables in prestressed steel structures. *Journal of Materials in Civil Engineering*, vol. 23, no.9, pp.1265-1271.

Costello, G. A. (1997): *Theory of wire rope*. 2nd Ed, Springer-Verlag, New York.

Elata, D.; Eshkenazy, R.; Weiss, M. P. (2004): The mechanical behavior of a wire rope with an independent wire rope core. *International Journal of Solids and Structures*, vol.41, no.5-6, pp.1157-1172.

Feyrer, K. (2007): *Wire rope-Tension, Endurance, Reliability*. Springer- Verlag, Berlin Heidelberg.

Hobbs, R. E.; Raoof, M. (1983): Interwire slippage and fatigue prediction in stranded cables for TLP tethers. *Proceedings of the 3rd International Conference on Behaviour of Offshore Structures* (*BOSS 82*) New York, USA, 1982, vol.2, pp.77-99.

Huang, N. C. (1978): Finite extension of an elastic strand with a central core. *Journal of Applied Mechanics*, vol.45, no.4, pp. 852-858.

Jiang, W. (1995): **A** general formulation of the theory of wire ropes. *Journal of Applied Mechanics*, vol.62, no.3, pp.747-755.

Jiang, W. G.; Warby, M. K.; Henshall, J. L. (2008): Statically indeter minate contacts in axially loaded wire strand. *European Journal of MechanicsA/Solids*, vol.27, no.1, pp.69-78.

Love, A. E. H. (1944): *A treatise on the mathematical theory of elasticity*. Dover Publications, New York, pp. 381-398.

Nawrocki, A.; Labrosse, M. (2000): A finite element model for simple straight wire rope strands. *Computers and Structures*, vol.77, no.4, pp.345-359.

Peng, Y. X.; Zhu, Z. C.; Tong, M. M.; Chen, G. A.; Cheng, Y. H.; Li, T. Q.; Li, Y. L.; Ma, W; Wang, C. Q.; Liu, B. B. (2012): Thermo-stress coupling field of friction lining during high-speed slide of wire rope in a mine friction-drive hoist. *Proceedings of the Institution of Mechanical Engineers, Part C: Journal of Mechanical Engineering Science*, vol. 226, no. 9, pp. 2154-2167.

Ramsey, H. (1990): Analysis of interwire friction in multilayered cables under uniform extension and twisting. *International Journal of Mechanical Sciences,* vol.32 no.8, pp.709-716.

Sun, G. J.; Chen, Z. H.; Liu, Z. S. (2011): Analytical and experimental investigation of thermal expansion mechanism of steel cables. *Journal of Materials in Civil Engineering*, vol.23, no.7, pp.1017-1027.

Usabiaga, H.; Pagalday, J. M. (2008): Analytical procedure for modelling recursively and wire by wire stranded ropes subjected to traction and torsion loads. *International Journal of Solids and Structures*, vol.45, no.21, pp.5503-5520.

Velinsky, S. A. (1985): Analysis of Fiber-Core Wire Rope. *Journal of Energy Resources Technology*, vol.107, no.3, pp. 388-393.

Xia, G. P.; Zhang, Z.; Ye, Y. (2009): Analysis of Temperature Effects on Cable-stayed Suspension Bridge. *Journal of Wuhan University of Technology (Transportation Science & Engineering)*, vol. 33, no. 5, pp. 892-896.

Appendix:

The mathematical equation of helical units could be expressed as

$$\begin{cases} x_i(k) = {}^cR_i\cos[\theta_i + 2(k-1)\pi/m_i] \\ y_i(k) = {}^cR_i\sin[\theta_i + 2(k-1)\pi/m_i] \\ z_i(k) = {}^cR_i\theta_i\tan\gamma_i \end{cases} \tag{A1}$$

where k is the position number denoting phase angle for rotational angle θ_i of the helical unit.

The axial strain ${}^c\xi_i$, increment of helical angle $\Delta\gamma_i$, tension ${}^cF_i$ torsion, ${}^cH_i$, bending moment ${}^cG_i^*$ and shearing force ${}^cN_i^*$ for helical units of the ith layer could be defined by parameters $\alpha\Delta T, \beta\Delta T$ and $\alpha_0\Delta T$,which are showed as

$${}^c\xi_i = {}^c\delta_i\alpha\Delta T + {}^c\zeta_i\beta\Delta T + {}^c\psi_i\alpha_0\Delta T, \tag{A2}$$

$$\Delta^c\gamma_i = {}^c\delta_{\Delta\gamma_i}\alpha\Delta T + {}^c\zeta_{\Delta\gamma_i}\beta\Delta T + {}^c\psi_{\Delta\gamma_i}\alpha_0\Delta T, \tag{A3}$$

$${}^cF_i = {}^c\delta_{F_i}\alpha\Delta T + {}^c\zeta_{F_i}\beta\Delta T + {}^c\psi_{F_i}\alpha_0\Delta T, \tag{A4}$$

$${}^cH_i = {}^c\delta_{H_i}\alpha\Delta T + {}^c\zeta_{H_i}\beta\Delta T + {}^c\psi_{H_i}\alpha_0\Delta T \quad , \tag{A5}$$

$${}^cG_i^* = {}^c\delta_{G_i^*}\alpha\Delta T + {}^c\zeta_{G_i^*}\beta\Delta T + {}^c\psi_{G_i^*}\alpha_0\Delta T \quad , \tag{A6}$$

$${}^cN_i^* = {}^c\delta_{N_i^*}\alpha\Delta T + {}^c\zeta_{N_i^*}\beta\Delta T + {}^c\psi_{N_i^*}\alpha_0\Delta T \quad , \tag{A7}$$

where

$${}^c\delta_i = {}^c\tilde{\delta}_i + {}^c\tilde{\phi}_i{}^c\delta_{\Delta R_i},\ {}^c\zeta_i = {}^c\tilde{\zeta}_i + {}^c\tilde{\phi}_i{}^c\zeta_{\Delta R_i},\ {}^c\psi_i = {}^c\tilde{\phi}_i{}^c\psi_{\Delta R_i} \quad ,$$

$${}^c\delta_{\Delta\gamma_i} = {}^c\tilde{\delta}_{\Delta\gamma_i} + {}^c\tilde{\phi}_{\Delta\gamma_i}{}^c\delta_{\Delta R_i},\ {}^c\zeta_{\Delta\gamma_i} = {}^c\tilde{\zeta}_{\Delta\gamma_i} + {}^c\tilde{\phi}_{\Delta\gamma_i}{}^c\zeta_{\Delta R_i},\ {}^c\psi_{\Delta\gamma_i} = {}^c\tilde{\phi}_{\Delta\gamma_i}{}^c\psi_{\Delta R_i},$$

$${}^c\delta_{F_i} = {}^c\tilde{\delta}_{F_i} + {}^c\tilde{\phi}_{F_i}{}^c\delta_{\Delta R_i},\ {}^c\zeta_{F_i} = {}^c\tilde{\zeta}_{F_i} + {}^c\tilde{\phi}_{F_i}{}^c\zeta_{\Delta R_i},\ {}^c\psi_{F_i} = {}^c\tilde{\psi}_{F_i} + {}^c\tilde{\phi}_{F_i}{}^c\psi_{\Delta R_i},$$

$${}^c\delta_{H_i} = {}^c\tilde{\delta}_{H_i} + {}^c\tilde{\phi}_{H_i}{}^c\delta_{\Delta R_i},\ {}^c\zeta_{H_i} = {}^c\tilde{\zeta}_{H_i} + {}^c\tilde{\phi}_{H_i}{}^c\zeta_{\Delta R_i},\ {}^c\psi_{H_i} = {}^c\tilde{\psi}_{H_i} + {}^c\tilde{\phi}_{H_i}{}^c\psi_{\Delta R_i},$$

$${}^c\delta_{G_i^*} = {}^c\tilde{\delta}_{G_i^*} + {}^c\tilde{\phi}_{G_i^*}{}^c\delta_{\Delta R_i},\ {}^c\zeta_{G_i^*} = {}^c\tilde{\zeta}_{G_i^*} + {}^c\tilde{\phi}_{G_i^*}{}^c\zeta_{\Delta R_i},\ {}^c\psi_{G_i^*} = {}^c\tilde{\psi}_{G_i^*} + {}^c\tilde{\phi}_{G_i^*}{}^c\psi_{\Delta R_i},$$

$${}^c\delta_{N_i^*} = {}^c\tilde{\delta}_{N_i^*} + {}^c\tilde{\phi}_{N_i^*}{}^c\delta_{\Delta R_i},\ {}^c\zeta_{N_i^*} = {}^c\tilde{\zeta}_{N_i^*} + {}^c\tilde{\phi}_{N_i^*}{}^c\zeta_{\Delta R_i},\ {}^c\psi_{N_i^*} = {}^c\tilde{\psi}_{N_i^*} + {}^c\tilde{\phi}_{N_i^*}{}^c\psi_{\Delta R_i}.$$

The total axial force and torsion of the single helical structure under temperature effect could be expressed [Cao et al(2012)] as

$$\begin{cases} T^*_{(n)} = EA_0(\alpha - \alpha_0\varsigma_0)\Delta T + \sum\limits_{i=1}^{n} m_i(F_i \sin\gamma_i + N^*_i \cos\gamma_i) \\ M^*_{(n)} = GJ^*_0\beta\Delta T + \sum\limits_{i=1}^{n} m_i[(H_i - N^*_i R_i)\sin\gamma_i + (G^*_i + F_i R_i)\cos\gamma_i] \end{cases}. \tag{A8}$$

According to Eq.A-2∼ Eq.A-8, the linear formulations are written as

$$\begin{cases} T^*_{(n)} = A_{(n)}\alpha\Delta T + B_{(n)}\beta\Delta T + C_{(n)}\alpha_0\Delta T \\ M^*_{(n)} = D_{(n)}\alpha\Delta T + E_{(n)}\beta\Delta T + F_{(n)}\alpha_0\Delta T \end{cases}, \tag{A9}$$

where

$$A_{(n)} = EA_0 + \sum_{i=1}^{n} m_i(\delta_{F_i}\sin\gamma_i + \delta_{N^*_i}\cos\gamma_i),$$

$$B_{(n)} = \sum_{i=1}^{n} m_i(\zeta_{F_i}\sin\gamma_i + \zeta_{N^*_i}\cos\gamma_i),$$

$$C_{(n)} = -E\varsigma_0 A_0 + \sum_{i=1}^{n} m_i(\psi_{F_i}\sin\gamma_i + \psi_{N^*_i}\cos\gamma_i),$$

$$D_{(n)} = \sum_{i=1}^{n} m_i[(\delta_{H_i} - \delta_{N^*_i}R_i)\sin\gamma_i + (\delta_{G^*_i} + \delta_{F_i}R_i)\cos\gamma_i],$$

$$E_{(n)} = GJ^*_0 + \sum_{i=1}^{n} m_i[(\zeta_{H_i} - \zeta_{N^*_i}R_i)\sin\gamma_i + (\zeta_{G^*_i} + \zeta_{F_i}R_i)\cos\gamma_i],$$

$$F_{(n)} = \sum_{i=1}^{n} m_i[(\psi_{H_i} - \psi_{N^*_i}R_i)\sin\gamma_i + (\psi_{G^*_i} + \psi_{F_i}R_i)\cos\gamma_i].$$

According to BC1, the axial and rotational thermal expansion coefficients of single helical structure could be simply expressed by

$$\alpha = \chi_{(n)}\alpha_0, \tag{A10}$$

$$\beta = o_{(n)}\alpha_0, \tag{A11}$$

where ratios of axial and rotational thermal expansion coefficients $\chi_{(n)}$ and $o_{(n)}$ under BC1 are respectively expressed as

$$\chi_{(n)} = -\frac{C_{(n)}E_{(n)} - F_{(n)}B_{(n)}}{A_{(n)}E_{(n)} - D_{(n)}B_{(n)}}, \tag{A12}$$

$$o_{(n)} = -\frac{C_{(n)}D_{(n)} - F_{(n)}A_{(n)}}{B_{(n)}D_{(n)} - E_{(n)}A_{(n)}}, \tag{A13}$$

According to BC2, the only axial thermal expansion coefficient of single helical structure could be simply expressed by

$$\alpha = \chi_{(n)}\alpha_0, \tag{A14}$$

where the ratio of axial thermal expansion coefficients under BC2 is formulated as

$$\chi_{(n)} = -C_{(n)}/A_{(n)} \tag{A15}$$